

“Boron + vacancy” complexes on the hydrogenated diamond surface C(100)-(2×1)

Anna I. Digurova^a, Natalia A. Lvova^{a,b}✉

^a Moscow Institute of Physics and Technology (National Research University),
9, Institutskiy per., Dolgoprudny, Moscow Region, 141701 Russian Federation;

^b Technological Institute for SuperHard and Novel Carbon Materials,
7a, Tsentralnaya St., Troitsk, Moscow region, 108840 Russian Federation

✉ nlvova@tisnum.ru

Abstract: The paper presents the results of quantum-chemical modeling of structural and electronic states of “boron + vacancy” complex defects on the hydrogenated and clean diamond surface, with a variation in the position of BV complexes in the upper six surface layers. Neutral, positive and negatively charged states of the complexes are considered. Two different positions of impurity and intrinsic defects in the composition of the BV complex have been considered for the third and fourth layers: under the dimer row and between the rows. The influence of the surface passivation on the position of BV complexes on the energy scale is analyzed. It has been found that hydrogenation of the surface leads to a change in the configuration of the most stable BV complex. The formation of a local graphite-like structure with π -conjugation is the main stabilizing factor for the defect structures, regardless of the considered charge state. It was shown that the distribution of the spin density of the studied negative BV complexes located directly in the near-surface layers of the clean and hydrogenated surface is similar to the spin properties of complexes in the bulk of diamond.

Keywords: diamond surface C(100)-(2×1); quantum chemical modeling; impurity defects; vacancies.

For citation: Digurova AI, Lvova NA. “Boron + vacancy” complexes on the hydrogenated diamond surface C(100)-(2×1). *Journal of Advanced Materials and Technologies*. 2021;6(4):256-266. DOI: 10.17277/jamt.2021.04.pp.256-266

Комплексы «бор + вакансия» на гидрированной поверхности алмаза C(100)-(2×1)

А. И. Дигурова^a, Н. А. Львова^{a,b} ✉

^a Московский физико-технический институт,
пер. Институтский, 9, Долгопрудный, Московская обл., 141701 Российская Федерация;

^b Технологический институт сверхтвердых и новых углеродных материалов,
ул. Центральная, 7а, Москва, Троицк, 108840 Российская Федерация

✉ nlvova@tisnum.ru

Аннотация: Представлены результаты квантово-химического моделирования структурных и электронных состояний комплексных дефектов «бор + вакансия» на гидрированной и чистой поверхности алмаза, при вариации положения BV комплексов в верхних шести приповерхностных слоях. Рассмотрены нейтральные, положительные и отрицательно заряженные состояния комплексов. Для третьего и четвертого слоев рассматривались два различных положения примесного и собственного дефектов в составе BV комплекса: под димерным рядом и в междурядье. Проанализировано влияние пассивации поверхности на положение BV комплексов на энергетической шкале. Обнаружено, что гидрирование поверхности приводит к изменению конфигурации наиболее стабильного BV комплекса. Показано, что формирование локальной графитоподобной структуры с π -сопряжением является основным стабилизирующим фактором для рассмотренных дефектных структур, независимо от рассмотренного зарядового состояния. Обнаружено, что распределение спиновой плотности большинства исследованных отрицательных BV^- комплексов, находящихся непосредственно в приповерхностных слоях чистой и гидрированной поверхности, подобны спиновым свойствам комплексов в объеме алмаза.

Ключевые слова: поверхность алмаза C(100)-(2×1); квантово-химическое моделирование; примесные дефекты; вакансии.

Для цитирования: Digurova AI, Lvova NA. “Boron + vacancy” complexes on the hydrogenated diamond surface C(100)-(2×1). *Journal of Advanced Materials and Technologies*. 2021;6(4):256-266. DOI: 10.17277/jamt.2021.04. pp.256-266

1. Introduction

“Impurity + vacancy” complexes in diamond have attracted considerable attention since the 1970s. The data of experimental and theoretical studies accumulated to date indicate the possibility of using “nitrogen + vacancy” complexes (NV centers) for measurements on nanoscale of various physical quantities; for quantum information processing at room temperature; as biomarkers in medicine. Since the optical activity of NV centers is directly related to the distance between defects and the surface of diamond particles, the use of complexes located in the near-surface layers is promising for achieving the highest resolution in measurements at the nanoscale [1, 2]. “Boron + vacancy” complexes (BV complexes) are considered as alternatives to NV defects. However, experimentally and theoretically, near-surface BV complexes remain poorly studied in comparison with defects in the bulk of diamond. In this regard, quantum-chemical modeling of BV complexes on the diamond surface is of considerable interest.

It is known that the most stable position in diamond is boron as a substitutional impurity leading to *p*-type conductivity [3]. The symmetry of an acceptor defect as a substitutional impurity in hole-type diamond was experimentally studied earlier [4] by infrared spectroscopy using uniaxial compression. The changes in the position of the spectral peaks were explained by the destruction of the tetrahedral symmetry of the T_d defect under deformation conditions. Later, the results of studying the electrical properties (conductivity and Hall effect) and neutron activation analysis showed that boron is the most probable impurity forming an acceptor level (0.37 eV above the valence band edge) [5]. The tetrahedral symmetry of a negatively charged boron atom in the position of carbon atom substitution in the diamond lattice was experimentally determined by X-ray photoelectron diffraction [6]. For the nearest environment of the boron atom in the neutral state, Jahn–Teller relaxation is noted: one of the interatomic B–C distances is reduced by about 2 % compared to the others due to loosening of the electron density in one of the bonding orbitals [7, 8]. Thus, the symmetry of the neutral defect is trigonal (C_{3v}). The Jahn–Teller relaxation of the nearest environment of neutral impurity atoms B was experimentally proved in studies of boron-doped diamond by the method of Raman light scattering at low temperatures (6 K) [9], as well as by observing the Zeeman effect [10].

Theoretically, studies of single boron atoms and a number of “boron + vacancy” complexes in diamond were carried out by the method of quantum-chemical calculations using the density functional theory (DFT) [7, 8, 11, 12]. In [11], a boron impurity was studied near various faces of diamond nanoparticles. In [8], B_nV multicomplexes were investigated for the volume of diamond; later, the structure of the energy levels of BV centers in various charge states was investigated [12]. According to calculations, negatively charged BV^{-1} centers can be created using an external electric field; the ground state of such centers is triplet.

It is obvious that, according to DFT calculations, different coating of the diamond surface C(100)-(2×1) (hydrogen, fluorine, oxygen, hydroxyl groups, nitrogen) affects the properties of NV centers [13]. It is shown that the optical properties of NV centers located in the 7-th and deeper layers from the surface are similar to the properties of centers in the bulk of diamond. It was found that the proximity to the surface leads to fluctuations in the position of the energy levels in the ground and excited states of NV centers located in the second and deeper to 6-th layers; however, these centers are optically active [13].

A similar study for BV complexes in various charge states located in the near-surface layers was not performed previously. Earlier in our works [14, 15], neutral BV complexes were investigated in four layers near a clean diamond surface. Geometric and energy characteristics of various configurations were calculated, as well as the charge distribution in the immediate environment of defects [14]. It was determined that a stable BV complex is a state in which a boron atom replaces a carbon atom in the fourth layer, while a vacancy is in the third layer under the dimer row. A hexagonal “graphene-like” structure of atoms bonded by π -conjugation is formed on the surface [14]. Next, we simulated the adsorption properties of the most stable and metastable neutral BV complexes during the deposition of atomic hydrogen on the clean surface, as well as a comparison with the properties of the defect-free surface [15]. However, negatively charged BV complexes are of particular interest, since the structure of their energy levels in the ground and excited triplet states meets the necessary conditions for using as a working element for quantum computing (qubit) [16]. In addition, it is interesting to study the effect of the charge on the configuration of

the most stable defect on the surface (boron in the fourth layer, vacancy in the third layer under the dimer rows) and the properties of the surface hexagonal “graphene-like” structure. The effect of the complete coverage of the diamond surface with various elements and groups of atoms on the structure and properties of BV complexes in the near-surface layers was not studied previously either. It should be noted that modeling of the hydrogenated diamond surface is traditionally used to determine the overall passivation effect [17]. In addition, according to experimental studies, near the hydrogenated surface of the diamond, by applying an appropriate electrical potential difference, switching between charged and neutral charge states of the “nitrogen + vacancy” complexes can be achieved [18, 19]. Thus, the study of BV complexes in various charge states near the hydrogenated diamond surface is of interest for possible practical applications.

The aim of this work was the quantum-chemical simulation of BV complexes in the near-surface layers of the hydrogenated diamond surface C(100)-(2×1):H, as well as comparison with complexes on the clean surface. The geometric, electronic, and energy characteristics of various configurations were calculated by varying the position of the complexes in neutral, negatively and positively charged states. The studies were carried out using a cluster model, semi-empirical approximations, and calculation schemes that were previously successfully applied to simulate single vacancies and “impurity + vacancy” complexes in near-surface layers [14, 15, 20, 21].

2. Calculation method

The modeling of the clean reconstructed diamond surface C(100)-(2×1) was carried out on the C₂₄₄H₁₁₆ cluster using the semi-empirical PM3 method implemented in the MOPAC software package [22]. The original cluster contained 10 layers of carbon atoms. The dangling bonds of carbon atoms at the edges of the clusters were saturated with hydrogen atoms, according to the model of univalent pseudoatoms [23, 24]. The essence of this model can be summarized as follows: the valences of the boundary atoms of the cluster are saturated using monovalent atoms (called pseudoatoms). Monovalent atoms are usually chosen on the basis of close values of electronegativity of pseudo-atoms and cluster atoms. Thus, the deviation from the stoichiometric charge distribution for cluster atoms is minimized. To simulate the structure and properties of clusters based on silicon, germanium, or carbon, hydrogen atoms are usually chosen as monovalent

pseudoatoms. Technically, the optimization procedure for the cluster geometry consists of several successive stages consisting in free optimization of the position of hydrogen atoms bounding the cluster, while maintaining the symmetry of the ideal lattice for the main cluster atoms, followed by full optimization of cluster atoms while fixing the position of pseudoatoms [25].

Since this work uses the semi-empirical method for calculating the structure and properties of complex defects, it seems appropriate to give a brief description of it. A detailed description of semi-empirical quantum-chemical methods is contained in the review [26]. It is known that all calculations of systems consisting of many atoms are based on approximate solutions of the Schrödinger equation. Semi-empirical methods consider only the valence electrons of the system involved in the formation of chemical bonds; the electrons of the inner shells are included in the potential of the nucleus [26]. Most of the time in the Hartree–Fock–Roothan calculations by the methods “from first principles” is spent on the calculation and operations with integrals characterizing the Coulomb and exchange interactions between electrons. Various semi-empirical methods use simplifying assumptions about these integrals. Some of them are set to zero, while others are replaced by parameters taken from the experiment.

The MNDO (Modified Neglect of Diatomic Overlap) method [27] is based on the semi-empirical Neglect of Diatomic Differential Overlap (NDDO) method [28], where the product of two different atomic orbitals is taken to be zero when they are localized on different atoms. In the MNDO method, the expression for the electron energy of a many-particle system of nuclei and electrons includes the terms $H_{\mu\mu}$ and $H_{\mu\nu}$, which in this approximation are calculated as follows [26]:

$$H_{\mu\mu} = U_{\mu\mu} - \sum_{B \neq A} V_{\mu\mu B} ;$$

$$H_{\mu\nu} = - \sum_{B \neq A} V_{\mu\nu B} ,$$

where the orbitals of the μ , ν electrons are localized on the atom A; the energy of the orbital Φ_{μ} in the field of its own nucleus A and electrons of the inner shells:

$$U_{\mu\mu} = \left\langle \mu \left| -\frac{1}{2} \nabla^2 - \frac{Z_A}{r_{1,A}} \right| \mu \right\rangle .$$

The terms on the right-hand side of the equations for $H_{\mu\mu}$ and $H_{\mu\nu}$ are determined according to atomic

spectroscopic data and correspond to the one-electron two-center interaction between the Φ_μ , Φ_ν orbitals of atom A and the nucleus of atom B. The total energy of the many-particle system is the sum of the electron energy and the repulsive energy between the nuclei of atoms A and B:

$$E_{AB} = Z_A Z_B (s_A s_A | s_B s_B) \times \{1 + \exp(-\alpha_A R_{AB}) + \exp(-\alpha_B R_{AB})\},$$

where the α coefficients are parameterized for atoms separately. Parametrization of the MNDO approximation is based on experimental data on the main properties of molecules: heats of formation, geometry, the ionization potentials, dipole moments.

The PM3 and PM6 methods are modified methods of Neglect of Diatomic Differential Overlap (MNDO, Parametric Method Number 3, 6) [29, 30]. In these approximations, one more term is added to the expression for calculating the internuclear interaction, which can be interpreted as the Van der Waals attraction energy. In the PM3 approximation, the additional term is determined by the spherical Gaussian functions:

$$E_N(A, B) = E_N^{\text{MNDO}}(A, B) + \frac{Z_A Z_B}{R_{AB}} \times \left(\sum_k a_{kA} e^{-b_{kA}(R_{AB}-c_{kA})^2} + \sum_k a_{kB} e^{-b_{kB}(R_{AB}-c_{kB})^2} \right),$$

with a , b , and c being adjustable parameters. In the PM3 approximation, two Gaussian functions are used for one atom.

In the PM6 approximation, the nuclear interaction potential is written in the form [31] (x_{AB} , α_{AB} are adjustable parameters):

$$E_{AB} = Z_A Z_B (s_A s_A | s_B s_B) \times \{1 + x_{AB} \exp(-\alpha_{AB}(R_{AB} + 0.0003R_{AB}^6))\}.$$

The advantage of quantum chemistry semi-empirical methods over *ab initio* is that semi-empirical calculations require significantly less computer time, as well as the required amount of operative and external memory. In [32], the accuracy of some semi-empirical approximations and DFT methods in determining the formation energy of 1276 molecules was compared. The value of the average error (in absolute value) was determined as the difference (in kcal/mol) in the values of the calculated and experimentally determined energy of molecule formation. It was determined that the

average errors are 15.38, 6.54, 5.57, 6.69 kcal·mol⁻¹ for the MNDO, PM3, PM5, DFT methods, respectively [32].

In our previous articles [20, 21, 33], test calculations were carried out: modeling of mono- and divacancies in the upper layer of a clean diamond surface using a number of approximations (PM3, PM6, MNDO), as well as the reconstructed fully hydrogenated and fluorinated diamond surface C(100)-(2×1). Comparison of the results obtained with the theoretical calculations [34–36] and experimental works [37] made it possible to determine the PM3 approximation as the optimal one for the chosen calculation model. According to the calculations in [36], carried out by the DFT methods (periodic conditions), the energies of formation of neutral single mono- and divacancy are 2.97 and 1.28 eV, respectively. Thus, the difference in energies of clusters with two monovacancies or one divacancy should be equal to 4.66 eV. The use of the PM3 method made it possible to achieve the best agreement (0.12 eV per defect) with the difference between the formation energies of two single monovacancies located at a large distance from each other and one divacancy calculated in [36]. In addition, in the case of using the PM3 method, the geometric parameters of vacancies were closest to the data obtained as a result of DFT calculations of the same work. In connection with the above, to simulate complex BV defects, the PM3 approximation was used in this work.

At stationary points of the system, the average forces on atoms did not exceed 0.02 eV/Å. The total cluster energy, bond orders of atoms, population of atomic orbitals, molecular, localized orbitals were calculated. Point defects were simulated by removing a carbon atom from the cluster (vacancy defect) or replacing it with boron (impurity defect). When simulating the fully hydrogenated surface (Fig. 1), the cluster contained 24 additional H atoms adsorbed on the outer surface was used: each atom of the surface dimers formed a covalent bond with one hydrogen atom. The dimeric bond was retained, but the corresponding C–C bonds became single, in accordance with the literature data on the reconstructed hydrogenated surface [38, 39].

3. Results and Discussion

It was noted above that the Jahn–Teller relaxation for the nearest environment of an impurity boron atom in the neutral state in the diamond lattice was proved experimentally. A similar result for boron atoms in 5–6 layers of the diamond surface C(100)-(2×1)

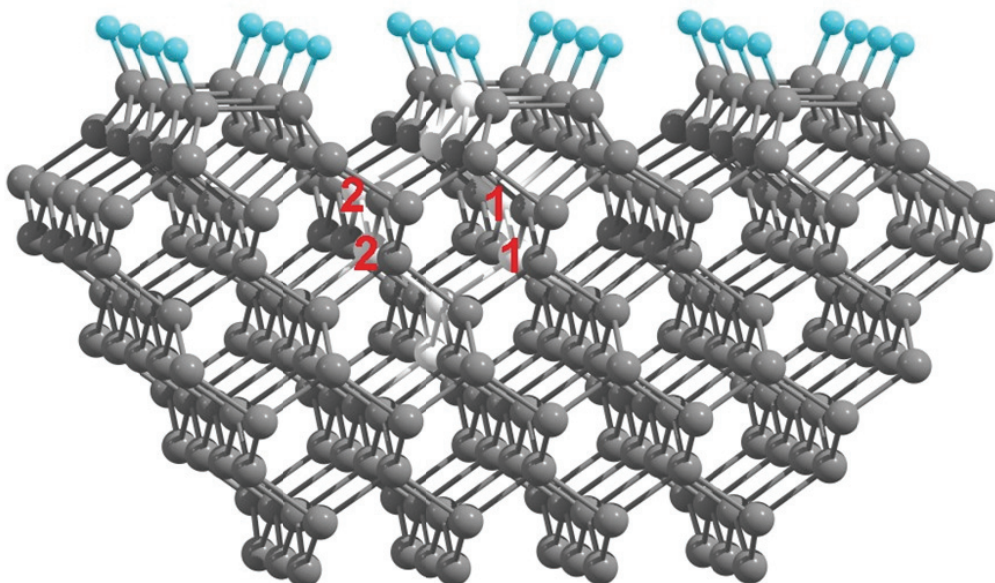


Fig. 1. Fragment of the $C_{244}H_{140}$ cluster simulating a surface with an ordered structure $C(100)-(2\times 1):H$ (During the calculations, the defects moved in layers 1–6. The carbon atoms replaced by boron atoms or vacancies are highlighted in light gray. The positions below the dimer rows and in the row spacing are designated by numbers 1 and 2, respectively. Hydrogen atoms saturating bonds going into the bulk are not shown)

was obtained in this work: three B–C bonds are 1.62 Å, the fourth bond is reduced (1.59 Å). Thus, the bond lengths for the ideal diamond lattice, for three equivalent bonds and for the shortened bond surrounded by a defect are in the ratio 1/1.05/1.03. This ratio is in agreement with the results of DFT calculations (for periodic conditions) in [7]: 1/1.03/1.02. Consequently, the use of the model cluster and the calculation scheme makes it possible to obtain the results that agree with the available experimental and theoretical data (qualitatively and quantitatively, respectively).

Using the MOPAC software package, the PM3 approximation, and the initial clusters $C_{244}H_{116}$ (clean surface) and $C_{244}H_{140}$ (hydrogenated surface), the energy, geometric, and electronic characteristics of the $C(100)-(2\times 1)$ surface were studied by varying the position of complex BV defects in the upper six near-surface layers. In all the cases, the intrinsic and impurity defects were located in neighboring lattice sites. For the third and fourth layers, two different positions of defects were considered: under the dimer row – 3 (1), 4 (1) – and between rows – 3 (2), 4 (2). The corresponding configurations are illustrated in Fig. 1.

16 combinations of complex BV defects were studied in neutral, negatively and positively charged states. Table 1 shows the energies of clusters containing the complex defect. The energy of clusters with the vacancy defect located as far as possible from the surface is taken as zero. In accordance with

the energy level diagram from [12], neutral, negatively, and positively charged BV complexes were considered in the states of a doublet, a “biradical” triplet, and a singlet, respectively. The exceptions were negatively charged complex 1 on a clean surface, as well as negatively charged complex 3 on a hydrogenated surface, for which the lowest energy state was found, corresponding to a system of molecular orbitals (MO), twice occupied by electrons with oppositely directed spins.

Fig. 2*a, b* illustrates the energy dependence of $C_{242}H_{116}B$ clusters (clean surface) on the defect position in the near-surface layers; Fig. 2*c, d* illustrates similar dependencies for $C_{242}H_{140}B$ clusters (hydrogenated surface). The position of the complex was determined by the layer number L containing the boron atom (Fig. 2*a, c*) or the vacancy (Fig. 2*b, d*). When constructing the graphs for each L , the BV complexes corresponding to the lowest value of the cluster energy were selected. On the clean surface, the lowest energy is possessed by defect 1 (boron in the fourth layer, vacancy in the third layer under the dimer row). On the hydrogenated surface, the most stable defect is the BV complex located directly in the upper layers: boron in the second layer, vacancy in the first (complex 3). It should be noted that the obtained results do not depend on the charge state of the defect. Stable BV complexes are illustrated in Fig. 3. To elucidate the reasons for this difference, these states were considered in more detail, the description of which is contained in Table 2.

Table 1. The value of the total energy E of clusters $C_{242}H_{116}B$ (clean surface) and $C_{242}H_{140}B$ (hydrogenated surface) for various configurations of the “boron + monovacancy” complex

Complex number, K	Layer number L		BV^0		BV^-		BV^+	
	with boron	with vacancy	clean surface, E , eV	hydrogenated surface, E , eV	clean surface, E , eV	hydrogenated surface, E , eV	clean surface, E , eV	hydrogenated surface, E , eV
1	4 (1)	3 (1)	-7.57	-1.25	-6.17	-1.09	-6.81	-0.71
2	2	3 (1)	-5.35	-1.52	-6.03	-1.65	-4.63	-1.62
3	2	1	-4.83	-5.03	-4.30	-3.11	-4.35	-4.28
4	3 (1)	2	-1.78	-0.57	-1.03	-0.75	-1.80	-0.12
5	1	2	-2.89	-2.19	-4.25	-1.43	-2.52	-1.65
6	6	5	-0.81	-0.34	-0.22	-0.19	0.00	0.06
7	3 (2)	2	-2.00	-1.95	-0.77	-0.67	-1.05	-0.70
8	5	4 (2)	-0.57	-0.17	-0.35	-0.35	-0.03	0.07
9	3 (2)	4 (2)	-1.65	-1.11	-0.91	-0.77	-0.88	-0.73
10	3 (1)	4 (1)	-0.93	0.06	-0.51	0.05	-0.48	0.21
11	4 (2)	3 (2)	-0.59	0.55	0.10	0.12	0.24	0.88
12	4 (1)	5	-0.17	0.10	-0.12	-0.09	0.43	0.31
13	5	4 (1)	-0.38	-0.20	-0.34	-0.26	-0.54	0.15
14	4 (2)	5	-0.98	-0.38	-0.33	-0.24	-0.57	-0.39
15	2	3 (2)	0.28	0.52	-1.33	0.39	-0.92	0.61
16	5	6	0.00	0.00	0.00	0.00	0.00	0.00

Note: The numbers in brackets correspond to the positions of the defects under the dimer row (1) and between the rows (2).

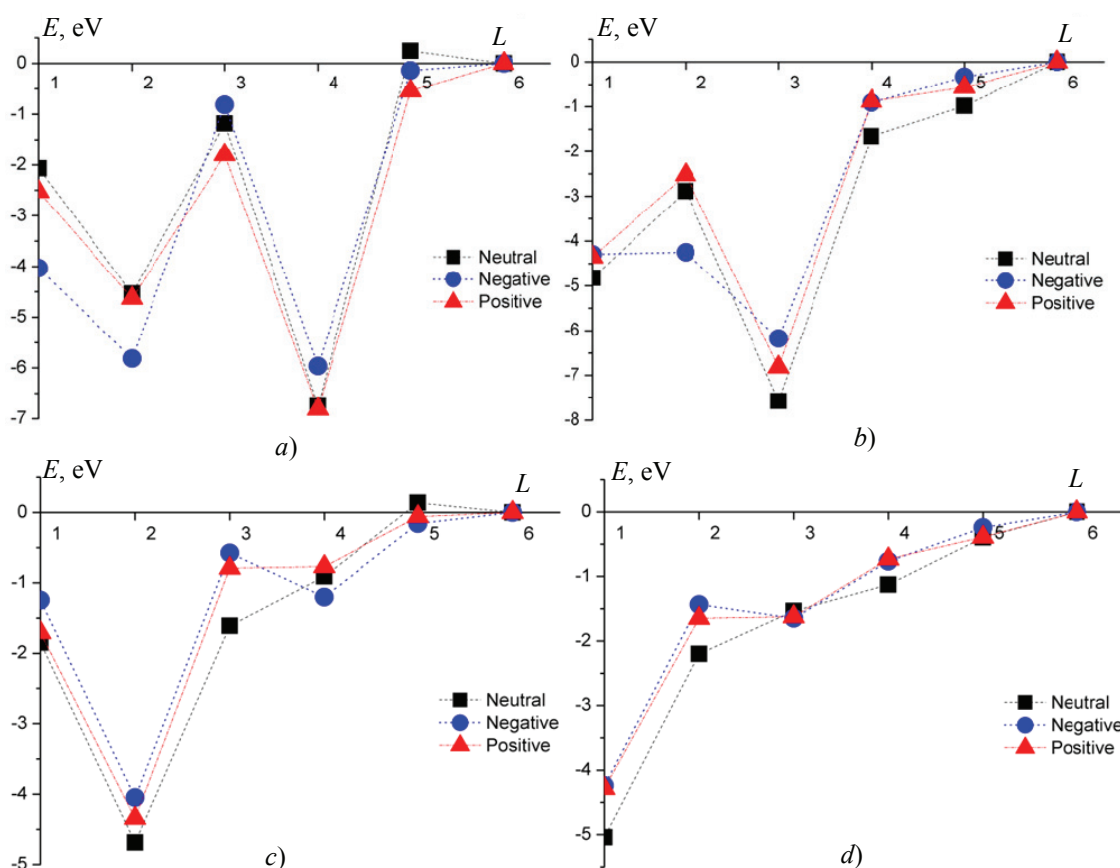


Fig. 2. The dependency of the total energy E of $C_{242}H_{116}B$ (with the clean surface) (a, b) and $C_{242}H_{140}B$ (with the hydrogenated surface) (c, d) clusters on the layer number L containing the boron atom (a, c) or the vacancy (b, d), for the most stable BV centers in different charge states

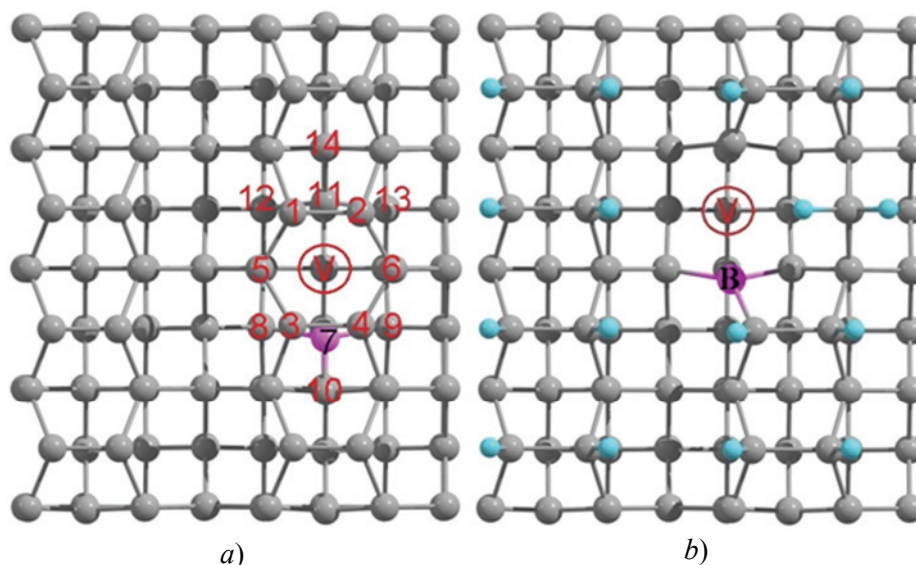


Fig. 3. The most stable BV complexes:
a – clean surface, complex 1; *b* –hydrogenated surface, complex 3
 (In the left figure, carbons atoms C1–C6 and C8–C14 are numbered 1–6 and 8–14, respectively.
 The boron atom B7 is marked with 7 and highlighted in pink)

Table 2. The calculations results of electronic and geometric parameters of stable BV complexes (to Fig. 3*a*)

Defect Surface	BV ⁰		BV ⁻		BV ⁺	
	Clean	Hydrogenated	Clean	Hydrogenated	Clean	Hydrogenated
1	2	3	4	5	6	7
Defect number				1		
B layer				4		
V layer				3		
<i>b.o.</i> (C1–C2)	1.37	0.92	1.37	0.93	1.37	0.92
<i>d</i> (C1–C2), Å	1.43	1.62	1.44	1.61	1.43	1.59
<i>b.o.</i> (C3–C4)	1.35	0.92	1.34	0.93	1.35	0.96
<i>d</i> (C3–C4), Å	1.44	1.60	1.44	1.61	1.44	1.58
<i>b.o.</i> (C1–C5)	1.39	1.00	1.38	1.00	1.39	0.98
<i>d</i> (C1–C5), Å	1.40	1.50		1.49		1.50
<i>b.o.</i> (C3–C5)	1.39	0.98	1.40	1.00	1.40	0.97
<i>d</i> (C3–C5), Å	1.40	1.52		1.49		1.51
<i>b.o.</i> (B7–C8)	1.01	0.99	0.96	0.97	1.01	1.01
<i>d</i> (B7–C8), Å	1.51	1.53	1.54	1.54	1.51	1.52
<i>b.o.</i> (B7–C10)	0.99	0.98	0.93	0.95	1.00	0.99
<i>d</i> (B7–C10), Å	1.51	1.53	1.58	1.57	1.50	1.52
<i>b.o.</i> (C11–C12)	1.00	0.97	0.98	0.99	1.05	0.98
<i>d</i> (C11–C12), Å	1.48	1.51	1.50	1.50	1.46	1.51
<i>b.o.</i> (C11–C14)	1.01	0.98	0.97	0.99	1.06	0.99

Continuation of the table 2

	1	2	3	4	5	6	7
d (C11–C14), Å	1.46	1.50	1.52	1.50	1.45	1.49	
Q (C1, C2), e	–0.02	–0.03	–0.01	+0.03	–0.06	–0.09	
Q (C3, C4), e	–0.02	–0.02	–0.03	+0.02	0.00	–0.08	
Q (C5, C6), e	–0.04	–0.01, –0.13	–0.02	–0.22	–0.04	+0.22	
Q (B7), e	+0.08	+0.08	+0.06	+0.09	+0.05	+0.04	
Q (C11), e	–0.15	+0.02	–0.42	–0.29	+0.42	+0.06	
S (C1, C2), e			0.03, 0		0.02		
S (C3, C4), e	0						
S (C5, C6), e			0.08, 0.72	–	0.31	–	–
S (C11), e	0.75				0.33		
S (B), e	0.01		0		0		

Note: B layer is the layer containing the boron atom; V layer is the layer containing the vacancy; $b.o.$ is bond order; d is interatomic distance; Q is charge; S is spin density.

Neutral complexes

Previously, neutral BV complexes on the clean reconstructed surface C(100)-(2×1) were studied in [14, 15] using the initial cluster C₁₉₅H₁₁₂ containing five layers of carbon atoms. It was found that the most stable configuration is “vacancy in the third layer, boron in the fourth layer under the dimer rows”, as well as the structure of the defect was analyzed. However, since the model cluster in [14] consisted of five layers of carbon atoms, which could partially affect the energy, geometric, and electronic characteristics of the defect, this paper briefly describes the similar stable defect 1 for the C₂₄₂H₁₁₆B cluster consisting of 10 carbon layers.

Defect 1 on the clean surface is the only one studied that forms the C1–C6 carbon structure from atoms of the first and second layers (Fig. 3a) united by common multicenter hybrid sp -orbitals (p -component is more than 90%). The formation of the π -bonded hexagonal (non-planar) structure similar to graphene is accompanied by a significant decrease in the cluster energy in comparison with other investigated defects. The total charge on C1–C6 atoms is –0.16 e (–0.14 e for the C₁₉₃H₁₁₂B cluster). In general, the data obtained for clusters consisting of 5 and 10 layers of carbon atoms are similar: the difference in the energies of clusters containing defects 1 and 2 is 2.35 and 2.22 eV for C₁₉₃H₁₁₂B and C₂₄₂H₁₁₆B, respectively.

Similar to NV complexes [21], the coating of the surface with hydrogen leads to the destruction of the

π -conjugation of the C1–C6 hexagon. The order of C1–C2, C1–C5 and similar bonds decreases to single, the corresponding interatomic distances increase in comparison with the clean surface; charge distribution changes (Table 2). As a result of these changes, complex 5 shown in Fig. 3b becomes the most stable.

Negatively charged complexes

For complex 1 on the clean surface, the lowest energy state corresponds to a system of molecular orbitals, twice occupied by electrons with oppositely directed spins. The main charge (–0.42 e) is localized on the C11 carbon atom of the fourth layer, which is in the nearest environment of the vacancy; the corresponding population of the orbitals increases from 4.15 (BV⁰) to 4.42 (BV[–]). In addition, an increase in the negative charge on the atoms of the surface dimers is noted (the maximum charge is –0.12 e). The doubly occupied HOMO, as well as HOMO-1 and HOMO-2, localized on the atoms of C1–C6 hexagon, are multicenter and consist almost entirely of C1–C6 p -orbitals (s -component is less than 10%) (Fig. 3a). Thus, C1–C6 hexagon retains the π -conjugation which consists of multicenter hybrid orbitals with a large p -component (more than 90%). The appearance of an additional electron density on C11 atom is accompanied by an increase in the population of the orbitals of boron atom (from 2.92 to 2.94), as well as C3 and C4 atoms of the dimer closest to boron (from 4.02 to 4.03), as compared to neutral complexes. Accordingly, the

value of the positive charge on the boron atom B7 decreases; the negative charge increases on C3, C4 atoms.

For complex 1, the “biradical” state was considered on the hydrogenated surface. Dimeric bonds C1–C2, C3–C4 are retained, but become single. The highest doubly occupied orbital becomes a multicenter MO, to which the hybrid orbitals of C11, C5, C6, and B7 atoms (*s*-component 30, 5, 5, 13 %, respectively) contribute. Half occupied energetically degenerated orbitals are localized on the atoms of the second layer in the composition of the surface hexagon C5, C6, as well as on the atom of the fourth layer C11. The “extra” electron density is distributed between C5, C6 and C11 atoms where the main spin density is also concentrated (Table 2).

It is also important to note that for negatively charged complexes 4–16, both on the clean and hydrogenated surface, the main spin density is distributed between the carbon atoms of the nearest environment of the vacancy. Thus, the spin properties of BV complexes located directly in the near-surface layers of the clean or passivated diamond surface are similar to the properties of complexes in the bulk of diamond.

Positively charged complexes

For positively charged defect 1, the singlet state was also considered, in which all MOs are pairwise occupied by electrons. The hexagonal graphene-like surface structure of C1–C6 is retained. The change in charge from negative to positive also does not significantly affect the configurations of hybrid MOs that bind C1–C6 atoms: the *p*-component is more than 90 %. However, unlike the negatively charged defect, MOs providing π -conjugation are located in the depths of the energy spectrum. The main positive charge (+0.42 e) is concentrated on C11 atom. Accordingly, the total population of C11 atomic orbitals decreases to 3.58, mainly due to the *p_z*-orbital. The total population of the orbitals of the boron atom remains almost unchanged (2.95).

As in the previous cases, there is no π -conjugation of the C1–C6 structure on the hydrogenated surface. Hybrid orbitals of C11, C5, C6 make almost the same contribution to the HOMO configuration, and a small contribution from the boron atom is also noted; *s*-components are equal to 18, 10, 10 and 5 %, respectively. The appearance of hydrogen on the surface leads to a significant redistribution of the electron density in the immediate environment of the defect: there is almost no charge on C11 atom; the population of atomic orbitals of

C11 increases to 3.94. A positive charge appears on the atoms of the second layer C5, C6; accordingly, the population decreases to 3.78.

It is also important to note that the change in the charge state (positive – neutral – negative) of BV complexes on the clean surface does not affect the atoms of the surface hexagon C1–C6, which indicates the stability of its locally graphitized structure.

In [40], the structure and energy stability of multi-vacancies in the bulk of diamond were calculated using the density functional theory. It was found that multi-vacancies, in the immediate environment of which structures of carbon atoms united by multicenter π -bonds are formed, are more stable in comparison with other configurations with the same number of absent atoms. The relaxation of dangling bonds in diamond is hindered by the influence of the framework of the surrounding covalent bonds. The tendency to form π -bonds is a sign of a certain degree of graphitization around some of the multi-vacancies, which in turn removes the non-bonding dangling orbitals, providing stability and possibly reduced reactivity of the corresponding voids [40]. The study carried out in this work has shown that a similar effect is also observed for the diamond surface.

4. Conclusion

The simulation of the clean C(100)-(2×1) diamond surface containing complex BV defects has shown that the most stable configuration, independent of the charge state, is the structure “vacancy in the third layer, boron in the fourth layer under dimer rows”. The analysis of MO configurations and electronic states of atoms in the immediate environment of complex near-surface defects, carried out in this work, allows us to conclude that local graphitization of the surface (formation of a hexagonal structure with π -conjugation) is the main factor stabilizing the position of complex BV defects on the energy scale. This conclusion is valid for all considered charge states of the complexes. Thus, structures of carbon atoms bonded by multicenter π -bonds in the immediate environment of point defects stabilize the configurations of defects both in the bulk and on the surface of the diamond. Hydrogenation of the surface leads to the disappearance of π -conjugation, and the BV complex located in the upper bilayer becomes the most stable.

The distribution of the spin density of the studied BV complexes located directly in the near-surface layers of the clean or hydrogen-passivated diamond surface is similar to the spin properties of the complexes in the bulk.

5. Funding

The work was financially supported by the Russian Foundation for Basic Research (project No. 18-29-19019).

6. Conflict of interests

The authors declare no conflict of interest.

References

- Nagl A, Hemelaar SR, Schirhagl R. Improving surface and defect center chemistry of fluorescent nanodiamonds for imaging purposes – a review. *Analytical and Bioanalytical Chemistry*. 2015;407(25):7521-7536. DOI:10.1007/s00216-015-8849-1
- Bernardi E, Nelz R, Sonusen S, Neu E. Nanoscale sensing using point defects in single-crystal diamond: recent progress on nitrogen vacancy center-based sensors. *Crystals*. 2017;7(5):124(1-20). DOI:10.3390/cryst7050124
- Blank VD, Kulnitskiy BA, Perezhogin IA, Terentiev SA, Nosukhin SA, Kuznetsov MS. Peculiarities of boron distribution in as-grown boron-doped diamond. *Materials Research Express*. 2014;1(3):035905. DOI:10.1088/2053-1591/1/3/035905
- Crowther PA, Dean PJ, Sherman WF. Excitation spectrum of aluminum acceptors in diamond under uniaxial stress. *Physical Review*. 1967;154(3):772-785. DOI:10.1103/PhysRev.154.772
- Collins AT, Williams AWS. The nature of the acceptor centre in semiconducting diamond. *Journal of Physics C: Solid State Physics*. 1971;4(13):1789-1800. DOI:10.1088/0022-3719/4/13/030
- Kato Y, Tsujikawa D, Hashimoto Y, Yoshida T, Fukami S, Matsuda H, et al. Three-dimensional atomic arrangement around active/inactive dopant sites in boron-doped diamond. *Applied Physics Express*. 2018;11(6):061302. DOI:10.7567/APEX.11.061302
- Goss JP, Briddon PR, Rayson MJ, Sque SJ, Jones R. Vacancy-impurity complexes and limitations for implantation doping of diamond. *Physical Review B*. 2005;72(3):035214. DOI:10.1103/PhysRevB.72.035214
- Goss JP, Briddon PR. Theory of boron aggregates in diamond: First-principles calculations. *Physical Review B*. 2006;73(8):085204. DOI:10.1103/PhysRevB.73.085204
- Kim H, Ramdas AK, Rodriguez S, Grimsditch M, Anthony TR. Spontaneous symmetry breaking of acceptors in “blue” diamonds. *Physical Review Letters*. 1999;83(20):4140-4143. DOI:10.1103/PhysRevLett.83.4140
- Kim H, Rodriguez S, Grimsditch M, Anthony TR, Ramdas AK. Jahn-Teller splitting and Zeeman effect of acceptors in diamond. *Physica B: Condensed Matter*. 1999;273-274:624-627. DOI:10.1016/S0921-4526(99)00589-X
- Barnard AS, Stenberg M. Substitutional boron in nanodiamond, bucky-diamond, and nanocrystalline diamond grain boundaries. *The Journal of Physical Chemistry B*. 2006;110(39):19307-19314. DOI:10.1021/jp0634252
- Kunisaki A, Muruganathan M, Mizuta H, Kodera T. First-principles calculation of a negatively charged boron-vacancy center in diamond. *Japanese Journal of Applied Physics*. 2017;56(4S):04CK02. DOI:10.7567/JJAP.56.04CK02
- Löfgren R, Pawar R, Öberg S, Larsson JA. The bulk conversion depth of the NV-center in diamond: computing a charged defect in a neutral slab. *New Journal of Physics*. 2019;21:053037. DOI:10.1088/1367-2630/ab1ec5
- Lvova NA, Ponomarev OV, Ananina OY, Ryazanova AI. Boron atoms in the subsurface layers of diamond: Quantum chemical modeling. *Russian Journal of Physical Chemistry A*. 2017;91(8):1451-1456. DOI:10.1134/S0036024417080180
- Ananina OYu, Ponomarev OV, Ryazanova AI, Lvova NA. Hemisorption of hydrogen on the diamond surface containing a “boron+vacancy” defect. *Nanosystems: Physics, Chemistry, Mathematics*. 2018;9(1):61-63. DOI:10.17586/2220-8054-2018-9-1-61-63
- Weber R, Koehl WF, Varley JB, Janotti A, Buckley BB, Van de Walle CG, et al. Quantum computing with defects. *Proceedings of the National Academy of Sciences*. 2010;107(19):8513-8518. DOI:10.1073/pnas.1003052107
- Bradac C, Gaebel T, Naidoo N, Rabeau JR, Barnard AS. Prediction and measurement of the size-dependent stability of fluorescence in diamond over the entire nanoscale. *Nano Letters*. 2009;9(10):3555-3564. DOI:10.1021/nl9017379
- Grotz B, Hauf MV, Dankerl M, Naydenov B, Pezzagna S, Meijer J, et al. Charge state manipulation of qubits in diamond. *Nature Communications*. 2012;3(1):729. DOI:10.1038/ncomms1729
- Pfender M, Aslam N, Simon P, Antonov D, Thiering G, Burk Set al. Protecting a diamond quantum memory by charge state control. *Nano Letters*. 2017;17(10):5931-5937. DOI:10.1021/acs.nanolett.7b01796
- Lvova NA, Ponomarev OV, Ryazanova A.I. Vacancies in the C(100)-(2×1) diamond surface layers. *Computational Materials Science*. 2017;131:301-307. DOI:10.1016/j.commatsci.2017.02.009.
- Ponomarev OV, Ryazanova AI, Lvova NA. Nitrogen-vacancy defects near the C(100)-(2×1) diamond surface. *Surface Science*. 2018;667:92-100. DOI:10.1016/j.susc.2017.10.003
- MOPAC2016, Version 16.158W, James JP Stewart, Stewart Computational Chemistry, Colorado Springs, CO, USA.
- Mikheikin ID, Abronin IA, Zhidomirov GM, Kazansky VB. The cluster model calculations of chemisorption and elementary acts of catalytic reactions. 1. Isotopic substitutions of hydrogen atoms of surface OH groups of silica gel. *Journal of Molecular Catalysis*. 1978;3(6):435-442. DOI:10.1016/0304-5102(78)85006-8
- Zhidomirov GM, Chuvylkin ND. Quantum-chemical methods in catalysis. *Russian Chemical Reviews*, 1986;55(3):153-164. DOI:10.1070/RC1986v055n03ABEH003178

25. Gorban A, Yanovsky A, Kolomoets S. Some details of hydrogen interaction with Si and Ge surfaces. *Physics of Low-Dimensional Structures*. 1998;910:65-76.
26. Gupta VP. Approximate molecular orbital theories. In: Gupta VP. *Principles and applications of quantum chemistry*. Academic Press; 2016. p.127-153. DOI:10.1016/B978-0-12-803478-1.00004-2
27. Dewar MJS, Thiel W. Ground states of molecules. 38. The MNDO method. Approximations and parameters. *Journal of the American Chemical Society*. 1977;99(15):4899-4907. DOI:10.1021/ja00457a004
28. Pople JA, Santry DP, Segal GA. Approximate self-consistent molecular orbital theory. I. Invariant procedures. *The Journal of Chemical Physics*. 1965; 43(10):S129-S135. DOI:10.1063/1.1701475
29. Stewart JJP. Optimization of parameters for semiempirical methods II. Applications. *Journal of Computational Chemistry*. 1989;10(2):221-264. DOI:10.1002/jcc.540100209
30. Stewart JJP. Optimization of parameters for semiempirical methods. III Extension of PM3 to Be, Mg, Zn, Ga, Ge, As, Se, Cd, In, Sn, Sb, Te, Hg, Tl, Pb, and Bi. *Journal of Computational Chemistry*. 1991;12(3):320-341. DOI:10.1002/jcc.540120306
31. Stewart JJP. Optimization of parameters for semiempirical methods V: Modification of NDDO approximations and application to 70 elements. *Journal of Molecular Modeling*. 2007;13(12):1173-1213. DOI:10.1007/s00894-007-0233-4
32. Stewart JJP. Comparison of the accuracy of semiempirical and some DFT methods for predicting heats of formation. *Journal of Molecular Modeling*. 2004;10(1):6-12. DOI:10.1007/s00894-003-0157-6
33. Lvova NA, Ananina OYu, Ryazanova AI. Fluorine and carbon fluoride interaction with a diamond surface: quantum-chemical modeling. *Computational Materials Science*. 2016;124:30-36. DOI:10.1016/j.commatsci.2016.07.014
34. Verwoerd WS. The adsorption of hydrogen on the (100) surfaces of silicon and diamond. *Surface Science*. 1981;108(1,2):153-168. DOI:10.1016/0039-6028(81)90364-2
35. Petrini D, Larsson K. A theoretical study of the energetic stability and geometry of hydrogen- and oxygen-terminated diamond (100) surfaces. *The Journal of Physical Chemistry C*. 2007;111(2):795-801. DOI:10.1021/jp063383h
36. Long R, Dai Y, Yu L, Jin H, Huang B. Study of vacancy on diamond (100) (2×1) surface from first-principles. *Applied Surface Science*. 2008;254(20):6478-6482. DOI:10.1016/J.APSUSC.2008.04.060
37. Pehrsson PE, Mercer TW. Oxidation of the hydrogenated diamond (100) surface. *Surface Science*. 2000;460(1-3):49-66. DOI:10.1016/S0039-6028(00)00494-5
38. Thoms BD, Owens MS, Butler JE, Spiro C. Production and characterization of smooth, hydrogen-terminated diamond C(100). *Applied Physics Letters*. 1994;65(2):2957-2959. DOI:10.1063/1.112503
39. Sque SJ, Jones R, Briddon PR. Structure, electronics, and interaction of hydrogen and oxygen on diamond surfaces. *Physical Review B*. 2006;73(8):085313. DOI:10.1103/PhysRevB.73.085313
40. Laszlo I, Kertesz M, Slepetz B, Gogotsi I. Simulations of large multi-atom vacancies in diamond. *Diamond and Related Materials*. 2010;19(10):1153-1162. DOI:10.1016/j.diamond.2010.05.001

Информация об авторах / Information about the authors

Дигурова Анна Ильинична, аспирант, ФГБОУ ВО «Московский физико-технический институт (национальный исследовательский университет)», Долгопрудный, Московская обл., Российская Федерация; ORCID 0000-0003-1974-6585; e-mail: ryazanova@phystech.edu

Львова Наталья Анатольевна, кандидат физико-математических наук, доцент, ведущий научный сотрудник, ФГБНУ «Технологический институт сверхтвердых и новых углеродных материалов», Троицк, Москва, Российская Федерация; ORCID 0000-0002-3230-7272; e-mail: nlvova@tisnum.ru

Anna I. Digurova, Postgraduate, Moscow Institute of Physics and Technology (National Research University), Dolgoprudny, Moscow Region, Russian Federation; ORCID 0000-0003-1974-6585; e-mail: ryazanova@phystech.edu

Natalia A. Lvova, Cand. Sc. (Physics and Mathematics), Assistant Professor, Leading Researcher, Technological Institute for SuperHard and Novel Carbon Materials, Troitsk, Moscow region, Russian Federation; ORCID 0000-0002-3230-7272; e-mail: nlvova@tisnum.ru

Received 29 September 2021; Accepted 16 November 2021; Published 28 December 2021



Copyright: © Digurova AI, Lvova NA, 2021. This article is an open access article distributed under the terms and conditions of the Creative Commons Attribution (CC BY) license (<https://creativecommons.org/licenses/by/4.0/>).